Structural and Dynamic Investigations of Unstretched and Stretched Ultrahigh Molecular Weight Polyethylene Films. 1-Pyrenyl Attachment by Bombardment with 4.5 MeV Protons and Irradiation with eV Range Photons

Chuping Luo,[†] Noel A. Guardala,[‡] Jack L. Price,[‡] Ivan Chodak,[§] Oscar Zimerman,[†,||] and Richard G. Weiss*[,†]

Department of Chemistry, Georgetown University, Washington, D.C., 20057-1227; Naval Surface Warfare Center, Carderock Division, 9500 MacArthur Boulevard, West Bethesda, Maryland 20817; and Polymer Institute, Slovak Academy of Sciences, 842 36 Bratislava, Slovak Republic

Received February 13, 2002; Revised Manuscript Received April 8, 2002

ABSTRACT: Several structural and dynamic properties of unstretched and stretched ultrahigh molecular weight polyethylene (**UHMWPE**) films, as well as **UHMWPE** films doped with pyrene (**Py/UHMWPE**) and either irradiated with UV−vis (eV range) photons or bombarded with 4.5 MeV protons, have been investigated. X-ray diffraction patterns of the three-dimensional orthorhombic crystal structure of a uniaxially stretched **UHMWPE** film, prepared by the gel technique, have been completely indexed for the first time. A minor monoclinic crystalline component, whose importance depends on the draw ratio, is also present. Linear dichroism spectra of dopant pyrene molecules indicate that their long molecular axes are oriented to a smaller extent in highly stretched **UHMWPE** films than in polyethylene films of much lower crystallinity and draw ratios. When **UHMWPE** films were stretched, the heat of melting was unchanged, but the melting temperature increased. Stretched films bombarded with 4.5 MeV protons exhibited lower heats of melting and melting temperatures than unstretched bombarded films. When **Py/UHMWPE** films were bombarded with 4.5 MeV protons or irradiated with >300 nm photons under oxygen-free conditions, 1-pyrenyl groups were attached covalently to polymer chains, yielding **Py-UHMWPE**. Diffusion of *N,N*-dimethylaniline (**DMA**) in to and out of **Py-UHMWPE** films was followed in real time by fluorescence intensity changes. In unstretched films, at least two parallel diffusion pathways appear to operate. The activation energies for diffusion of **DMA** in unstretched **Py-UHMWPE** are larger than those in stretched **Py-UHMWPE** or in other types of polyethylene films. The results are discussed in terms of the structural differences between unstretched and stretched **UHMWPE** and other polyethylene types.

Introduction

Ultrahigh molecular weight polyethylene (**UHMWPE**, $M_w > 10^6$) is manufactured by a slurry process with a hydrocarbon diluent using a heterogeneous Ziegler−Natta catalyst.[1] The very high molecular weights and lack of chain branches enable **UHMWPE** fibers and films to be drawn to >100 times their original lengths if special procedures are applied, yielding very high modulus (70−200 GPa) materials[2] that have been used for several applications where strength, light weight, malleability, or inertness to moisture are important (e.g., fishing nets, and bulletproof vests).[3] However, the specific mechanical properties of **UHMWPE** depend strongly on several features unique to the chain-extended microstructure, some of which are not well understood.[4] The microstructure of **UHMWPE** has been probed by ESR,[5] solid-state ^{13}C NMR,[6] Raman spectroscopy,[7] and, especially, X-ray diffraction.[8] Others[9] and we[10] have employed photophysical methods to investigate local morphological changes in polymer films, including other types of polyethylene. However, to the best of our knowledge, **UHMWPE** has not been investigated in this way.

Here, we use static and dynamic spectroscopic and photophysical techniques to probe *specific* sites within unstretched and uniaxially stretched **UHMWPE** films that contain either doped pyrene (**Py**) molecules (**Py/UHMWPE**) or covalently attached 1-pyrenyl groups (**Py-UHMWPE**). The long singlet excited-state lifetime, high fluorescence efficiency, sensitivity to local polarity,[11] and ease of excimer and exciplex formation of pyrene and alkylated pyrenes make them attractive probes to study dynamic processes[12] in and of polymers,[12a,b] micelles,[12d] and other microheterogeneous media.[12d−g] Covalent attachment of 1-pyrenyl groups in **Py/UHMWPE** has been achieved by bombardment with 4.5 MeV proton beams and by irradiation with eV range (>300 nm) photons. A small organic molecule that is also a contact quencher of pyrenyl excited singlet states,[10a−d] *N,N*-dimethylaniline (**DMA**), has been diffused into and out from **Py-UHMWPE** films. Diffusion coefficients for each process have been calculated according to a modified form of Fick's second law[10g,h,13] and temporal changes in fluorescence intensity from the unstretched and stretched films. These results are complemented by measurements that address ensemble *average* properties of **UHMWPE** microstructure (i.e., linear dichroism spectra of stretched **Py/UHMWPE** films) and bulk properties (i.e., X-ray diffraction and differential scanning calorimetry measurements).

The data have been used to extract information concerning the microstructure of **UHMWPE**, the nature

[†] Georgetown University.
[‡] Naval Surface Warfare Center.
[§] Slovak Academy of Sciences.
[||] Current address: Edge Biosystems, 19208 Orbit Drive, Gaithersburg, MD.

10.1021/ma020235q CCC: $22.00
Published on Web 05/10/2002

of guest sites within it, and the changes that occur when its films are stretched uniaxially.

Experimental Section

Materials. Ultrahigh molecular weight polyethylene powder from DSM, Holland (Stamilan UH, $M_w \sim 2.8 \times 10^6$) was used as received. Pyrene (Aldrich, 99%) was recrystallized from benzene, passed through an alumina column using benzene as eluant, and recrystallized twice from ethanol: mp 148.6−149.1 °C (lit. mp 149−150 °C).[14] *N*,*N*-Dimethylaniline (**DMA**; Aldrich, 99%) was distilled, saturated with N_2, and stored in a refrigerator until being used. Methanol (EM Science, HPLC grade), ethanol (EM Science, HPLC grade), xylenes (Baker analyzed) and chloroform (Fisher, HPLC grade) were used as received.

Instrumentation. Unless indicated otherwise, experiments were performed at room temperature. UV−visible spectra were measured using a dual-beam Perkin-Elmer Lambda-6 UV/vis spectrophotometer. Absorption spectra were recorded at three different positions on each film. To obtain linear dichroic absorption spectra, a pair of Glan Nicol prism polarizers was inserted in the optical paths of the spectrophotometer. Films were mounted vertically with respect to their direction of stretching. The spectra were recorded while the electric vector of the polarized light was parallel ($OD_{\parallel}$, vertical) and perpendicular ($OD_{\perp}$, horizontal) to the stretching direction of the films. Films were kept in a stationary position for the duration of each set of measurements. Results are based on polarized absorption spectra of three different parts of each film that were ratioed individually and averaged.

Fluorescence and excitation spectra were measured using a Spex Fluorolog III spectrofluorimeter. Both back-face and front-face emission and excitation spectra, for which the films were placed at a ca. 45° angle in the former and almost perpendicular to the exciting beam in the latter, were collected. Excitation spectra are corrected for detector response.

Temporal fluorescence decays were obtained with an Edinburgh Analytical Instruments model FL900 time-correlated single photon counting (TCSPC) system using H_2 as the lamp gas. Degassed film samples ($<10^{-5}$ Torr) in flattened quartz capillaries were aligned at ∼ 45 or ∼135° to the incident radiation. The emission was detected at a right angle from the incident light. An instrument response function was determined using Ludox as scatter and without polarizers. Data were collected in 2047 channels with $>10^4$ counts at the maxima of the decay curves unless indicated otherwise. Curve fitting and deconvolution were accomplished with a nonlinear least-squares routine using software supplied by Edinburgh Instruments. A range from time < 0 (a channel before the onset of the instrument-response signal) to at least 2 decades of decay from the peak channel was included in the analyses. Fits were considered acceptable when χ^2 values were < 1.5 and plots of residuals showed no systematic deviation from zero. The relatively high χ^2 values in some cases can be attributed to the scatter peaks.

Differential scanning calorimetry (DSC) on 4−5 mg film samples in closed aluminum pans was performed under a N_2 atmosphere using a TA 2910 DSC cell base interfaced to a TA Thermal Analyst 3100 controller. The heating rate was 5 °C/min, and the cooling rate was uncontrolled and depended on the difference between the sample and ambient temperatures.

X-ray diffraction (XRD) data were collected on a Rigaku RAPID/XRD image plate system with Cu Kα X-rays from a Rigaku generator. Data from three positions on each film were recorded and averaged unless indicated otherwise. Both sample and background data were collected over 4° in 2θ in steps of 0.02°. Data processing and analysis were performed using MDI (Jade version 5) software.[15]

Preparation of Undoped and Pyrene-Doped UHMWPE Films. Pyrene-doped or blank **UHMWPE** films were obtained from powder dissolved in hot xylenes by a gelation method.[16] To prepare undoped **UHMWPE** films, 0.98 g of **UHMWPE** powder and 80 mL of xylenes were stirred mechanically at reflux temperatures. After ca. 10 min, the "Weissenburg effect"[16] was observed, indicating gel formation. Stirring was stopped immediately, and the gel was poured into an aluminum foil tray. After 2−3 h, the solvent that had separated from the gel was removed with a pipet. The edges of the gelled film pieces were attached with staples to a piece of wood coated with aluminum foil. The pieces were dried slowly in the air for 2 weeks. Finally, the films were placed under vacuum for 1 week to remove traces of xylenes, and the surfaces of the films were rinsed with methanol, a nonswelling solvent for polyethylene.

Pyrene-doped **UHMWPE** films (**Py/UHMWPE**) were prepared as above except that 1.00 g of **UHMWPE** powder, 7.2 mg of pyrene, and 100 mL of xylenes were mixed initially. The concentration of pyrene incorporated into the **UHMWPE** film was 2.8×10^{-3} mol kg^{-1} based on the average film thickness (vide infra), the optical density at several positions, and the molar extinction coefficient of pyrene at 335 nm in hexane, 55 000 M^{-1} cm^{-1} (see Figure 1 of the Supporting Information).[17]

Film Thickness and Density.[18] Film thickness is reported as the average of five measurements at different spots using a Mitutoyo digimatic micrometer. Density was determined by placing a piece of film in a mixture of methanol and water at room temperature. Less-dense methanol or more-dense water was added dropwise, as needed, and mixed thoroughly until the film remained suspended. Thereafter, a 10.00 mL aliquot of the final liquid was transferred to a volumetric flask and weighed; its density, 0.960 ± 0.003 g cm^{-3} from three measurements, is that of the film.

Procedure for Stretching UHMWPE Films. A strip of film was held over a heating plate at 130−140 °C and stretched slowly. Thicker films allowed higher draw ratios (DR). Initially, films were drawn to DR = 4−9. Further stretching of an extended piece was performed as above, leading-to-draw ratios in the range 48−96.

Proton Bombardment of Py/UHMWPE Films. Unstretched **UHMWPE** and **Py/UHMWPE** films were exposed to uniform beams of 4.5 MeV protons from a 3 MV NEC Pelletron tandem accelerator.[19] An area of ca. 1 cm × 1 cm of the film was exposed to the proton beam projected through a 1 mm aperture in a tantalum foil. Fluences (F) were 10^{12} H$^+$ cm^{-2}, and the corresponding doses, calculated from eq 1,[20] were 2.7×10^4 Gy. E is the particle energy (MeV), ρ is the density of polyethylene (g cm^{-3}), and R is the stopping depth of 4.5 MeV protons in polyethylene.[20] The R value, 2.79×10^{-2} cm, was determined by the SRIM/TRIM software package,[21] which calculates the stopping range of ions with 10 eV-2 GeV/amu energies into materials using a full quantum mechanical treatment of ion−atom collisions.

$$\text{Dose} = (1.60 \times 10^{-10})\, FE/R\rho \qquad (1)$$

Following the exposures, **Py/UHMWPE** films were soaked in several batches of refluxing chloroform for a total of 1 month to remove unattached pyrene and other aromatic molecules (i.e., until no more pyrenyl-like molecules could be extracted). The surfaces were then washed with methanol and the films were dried under vacuum for >2 days to yield pyrenyl-attached films (**Py-UHMWPE-H**$^+$).

UV/Vis Irradiations of Unstretched Py/UHMWPE Films. One unstretched **Py/UHMWPE** film was placed in a closed Pyrex tube and purged with N_2 for ∼45 min, and another was flame-sealed in a flattened Pyrex capillary at < 10^{-5} Torr. Both were irradiated at >300 nm for 1 h on each face at a distance of ca. 5 cm from a Hanovia 450 W medium-pressure Hg arc. Following irradiations, the films were extracted and washed according to the procedures described for the proton-bombarded films to yield pyrenyl-attached films (**Py-UHMWPE-h*ν***).

Equilibrium Constants for Partitioning DMA between Methanol and Unstretched or Stretched (DR = 9) Py-UHMWPE-h*ν* Films. DMA partitioning constants between methanol and **Py-UHMWPE-h*ν*** films ($K_{par} = [\mathbf{DMA}]_{film}/[\mathbf{DMA}]_{methanol}$) were determined as described previously.[10a,c,g] A **Py-UHMWPE-h*ν*** film (thickness = 34 ± 7 μm for un-

Table 1. Selected Properties of UHMWPE and Some PE Films of Lower Crystallinity and Molecular Weight

polymer	draw ratio	M_w ($\times 10^5$)	density (g cm^{-3})	T_{mp}[c] (°C)	ΔH_m[d] (J g^{-1})	ΔH_c[e] (J g^{-1})	crystallinity[f] (%)
UHMWPE	1	28	0.960 ± 0.003	129	273 ± 2	160 ± 6	(95 ± 2) 85 ± 3
	9			129	275 ± 3	141 ± 5	(96 ± 1) 83 ± 3
	48			136	275 ± 3	152 ± 3	(96 ± 2) 87 ± 4
	1[b]			125	172 ± 5	169 ± 4	(60 ± 2) 61 ± 5
	9[b]			124	163 ± 6	130 ± 5	(56 ± 2) 50 ± 3
PE22[a]	1		0.916	112	82.9		22[g]
PE35[a]	1	1.1	0.917	116	100.1		35
PE38[a]	1	5.1	0.917	109	88.7		38[g]
PE42[a]	1		0.918	116	120.1		42[g]
[a]	1		0.945	129	203.1		73[g]

[a] Reference 10g. [b] Film bombarded with 4.5 MeV protons (fluence = 10^{12} cm^{-2}; dose = 2.7×10^4 Gy) and then stretched. [c] Melting point (±1 °C) as onsets of melting endotherms from first heating thermograms. [d] Heats of melting from first heating thermograms. [e] Heats of crystallization from first cooling thermograms. [f] From XRD; values from DSC in parentheses. [g] Crystallinities from XRD differ from the DSC values reported previously.[10g]

stretched or 33 ± 9 μm for stretched film (DR = 9)) was placed in the dark in 3.0 mL of an N_2-saturated 0.95 M **DMA**/MeOH solution for 1 day at 30−65 °C or 2 days at <30 °C. The film was removed from the liquid, washed rapidly with a small amount of methanol, and immersed in 3.0 mL MeOH for 1 day at room temperature to extract **DMA**. The concentration of **DMA** in the methanol was determined from Beer's law using the absorbance at 251 nm and 11 600 M^{-1} cm^{-1}as the molar extinction coefficient.[17] The concentrations of **DMA** in **Py-UHMWPE-h*ν*** (as mol kg^{-1} film) were then calculated from the weight of the film and its volume and density. Measurements were repeated in triplicate at each temperature.

Diffusion of DMA between Methanol and Unstretched and Stretched Py-UHMWPE-h*ν* Films. The same pieces of unstretched or stretched (DR = 9) **Py-UHMWPE-h*ν*** film used to determine partitioning constants were employed in the dynamic diffusion experiments. A film was placed in a flattened, closed quartz capillary that was immersed in a Pyrex cuvette filled with dodecane. The cuvette was placed in a thermostated cell holder in the spectrofluorimeter; temperature was maintained using a VWR 1140 circulating water bath. Temperature (15−60 °C) was measured with a thermistor that was in contact with the sample cuvette; readings were calibrated to temperatures of a thermometer directly in the dodecane liquid. For in-diffusion measurements, fluorescence intensity measurements (λ_{em} 377 nm; λ_{ex} 343 nm) were commenced immediately after a ca. 1.5 mL aliquot of an N_2-saturated 0.95 M **DMA**/MeOH solution, which had been equilibrated at the same temperature as the film, was introduced in the capillary. Measurements were made at frequencies of 0.2 s per point for the first 30 min, 0.5 s for the second 30 min, and 1 s per point thereafter. Usually, more than 10 000 points were collected, depending on the time needed to approach equilibrium. Out-diffusion measurements were made as above after removal of the **DMA** solution and replacement of it with 2.0 mL of temperature-equilibrated methanol. Each film was immobilized for the duration of each run; runs were repeated 2−4 times at each temperature.

Results and Discussion

Properties of UHMWPE Films. Percentages of film crystallinity were calculated from heats of melting determined from differential scanning calorimetry (DSC) thermograms and eq 2,[10g] as well as from X-ray diffraction (XRD) measurements of ratios of the areas of peaks related to amorphous and crystalline domains.[8,22] In eq 2, ΔH_m is the heat of melting of 1 g of polyethylene and ΔH_m*, 286 J/g, is the heat of melting of a single crystal of polyethylene.[23]

$$\% \text{ crystallinity} = 100\Delta H_m/\Delta H_m^* \qquad (2)$$

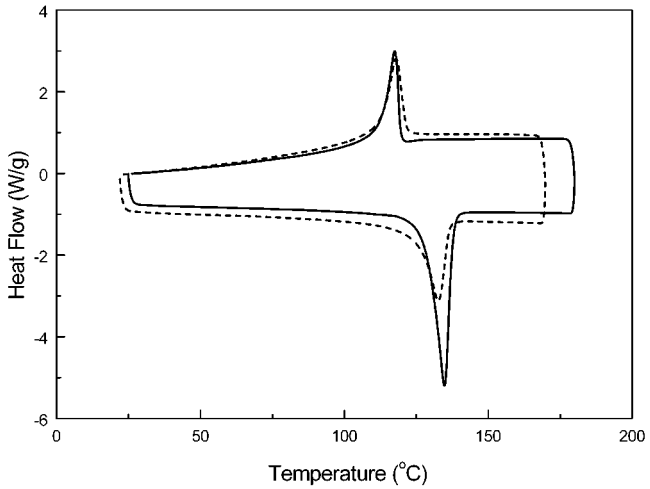

Figure 1. First heating (endotherms) and cooling (exotherms) DSC thermograms of unstretched **UHMWPE** before (—) and after (- - -) 4.5 MeV proton bombardment ($F = 10^{12}$ cm^{-2}; dose = 2.7×10^4 Gy).

(a) DSC Thermograms. Typical thermograms are shown in Figure 1, and the resulting data, including the melting temperatures of the crystalline portions, are collected in Table 1. As expected, ΔH_c (the heat of crystallization of 1 g of **UHMWPE**) and T_{fp} (the crystallization temperature) from first and second *cooling* thermograms are virtually identical, but the values of ΔH_m and T_{mp} (the melting temperature) from the second *heating* thermograms are always somewhat lower than the first (Figure 2 of the Supporting Information). Once melted, **UHMWPE** films do not resolidify to their original state at the cooling rates and after the short annealing periods employed; the amorphous content increases. For that reason, only values from first heating thermograms are presented unless indicated otherwise.

Values of ΔH_m of an undoped **UHMWPE** film before and after 4.5 MeV proton bombardment (**UHMWPE-H$^+$**) ($F = 10^{12}$ cm^{-2}) were 273 and 172 J/g, respectively, corresponding to 95% and 60% crystallinity. Proton bombardment appears to cause significant morphological changes in **UHMWPE**. The similarity of ΔH_c and ΔH_m values from first and second heating thermograms of **UHMWPE-H$^+$** (Table 1 and Figure 3 of the Supporting Information) and their difference from ΔH_c and ΔH_m values of **UHMWPE** point to chain cross-links as the

source of these changes.[3b,24] Cross-links may hold domains of melted chains in the same sites as before melting, allowing morphological changes induced by heating and cooling to be more reversible. However, some (if not all) of the cross-links must be broken as **UHMWPE-H**$^+$ is stretched, even to DR = 9: although T_{mp} does not change between the first and second heating thermograms, ΔH_m is reduced from 163 to 140 J/g; in addition, two shoulders at 131 and 149 °C on the main endotherm of the first melting transition are absent in the second scan.

The effect of draw ratio on crystallinity of an unbombarded **UHMWPE** film was investigated in greater detail (Table 1). As mentioned, thermograms of a film that was unstretched and stretched to DR = 9 were virtually indistinguishable. However, crystallinity (and heat of melting) of **UHMWPE** is reported to decrease as DR → 5 and then increase thereafter.[16] T_{mp} of a highly stretched (DR = 48) film was 7 °C higher than that observed from the DR = 1 and 9 films, and a shoulder was present at ca. 150 °C (i.e., on the high-temperature side of its main endotherm) in its heating thermogram (Figure 2 of the Supporting Information). Extreme stretching of **UHMWPE** films is known to unfold their lamellae into fully extended chains that are oriented parallel to the stretch direction.[8c] The absence of lamellar interfaces and the related greater London dispersion forces along chains makes their separation via melting more difficult.

(b) X-ray Diffraction Patterns. X-ray diffraction (XRD) has been widely employed to study the microstructure of different types of polyethylene.[8,22] Usually, XRD patterns consist of two sharp peaks at $2\theta = 23.9$ and 21.5° from $(110)_o$ and $(200)_o$ orthorhombic crystalline reflections, respectively. A weak, broad amorphous peak appears at $2\theta = 16-20°$.[8e,h,22] Crystallinity of **PE** films can be calculated from the ratio of the areas of the amorphous and orthorhombic diffractions.[8b,22,25,26] Diffraction from a minor monoclinic component (e.g., when films were prepared at < 20 °C[26]) and a pseudohexagonal phase (when films are left either under high pressure or at a temperature close to the melting point[8d,27]) of **UHMWPE** have also been observed in some cases. However, the monoclinic phase is not stable and can be transformed to the orthorhombic form when mechanical stress is applied to a film.

Radially averaged X-ray diffraction patterns of our **UHMWPE** films have been obtained with beams perpendicular to the film surface, but not parallel to them. As such, information about anisotropy of chain orientations along the *c*-axis is not available. The patterns from unstretched films consist of typical orthorhombic crystalline reflections (Figure 2).[4e,8e,h,22] A metastable monoclinic $(001)_m$ reflection, usually located at 19.4°,[6b,8g,22] is too weak to be detected during deconvolution of the XRD pattern.[15] The degree of crystallinity calculated for an unstretched **UHMWPE** film, 85%, is very close to the values reported previously for other **UHMWPE** samples,[1c,6a,22,26] but much lower than the value from DSC (Table 1). Measurements of crystallinity from DSC methods are usually higher than from XRD methods,[26] but values from the two methods follow the same trends and provide complementary information; both are model-driven to a certain extent and dependent on the values of parameters that are obtained in related systems. By either measure, the crystallinity of **UHMWPE** is significantly higher than that of even a "normal" high-density polyethylene, **PE73**,[10g] of similar density and melting temperature (Table 1). Although the microstructures of **UHMWPE** and **PE73** are very different, the vast majority of their polyethylene chains must be arranged in well-packed lamellae (vide infra).

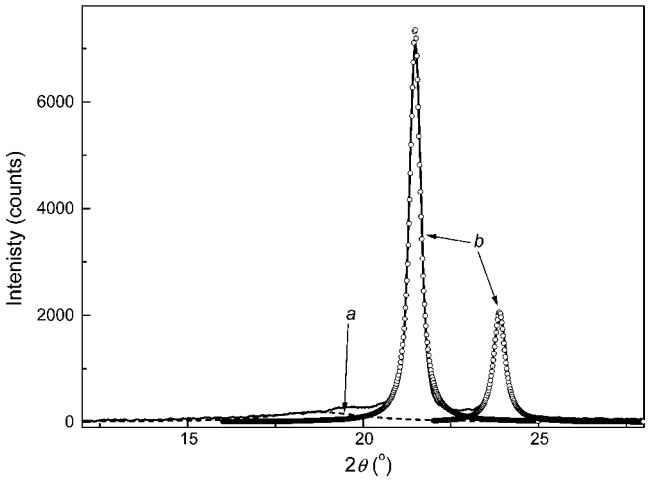

Figure 2. Deconvolution of the X-ray diffraction pattern of an unstretched **UHMWPE** film (—) into contributions from amorphous (- - -, *a*) and orthorhombic crystalline (○, *b*) portions. See text for details.

The azimuthal X-ray diffraction pattern of an unstretched **UHMWPE** film consists of two rings from reflections of $(110)_o$ and $(200)_o$ orthorhombic planes that are randomly oriented (Figure 3a).[22] Discrete spots and arcs in the X-ray pattern of a stretched (DR = 48) film (Figure 3b) demonstrate that its crystalline phase have become well oriented along the stretching axis. Because the axis of stretching was perpendicular to the X-ray beam and vertical with respect to the orientation of Figure 3b, discrete spots and arcs are located on the equatorial line and others are symmetrically disposed above and below the equator. The spots and arcs are indexed well to an orthorhombic cell of space group *Pnam* (Table 1 of the Supporting Information).[15] They resemble the crystal structure of waxes (determined by electron diffraction).[28] The spots on the equatorial line between 10 and 100° have been well indexed to the set of orthorhombic planes $(hkl)_o$ with $l = 0$.[8d,e,22] However, the off-equatorial diffraction arcs do not appear to have been detected from **UHMWPE** previously. They are from $(hkl)_o$ planes with $l \neq 0$.[15]

The effect of draw ratio on the XRD patterns from **UHMWPE** was probed in some detail. A small sharp peak at 19.5°, due to the $(001)_m$ reflection,[8g,22] increases up to DR = 9 and then becomes indistinguishable from the much stronger orthorhombic $(110)_o$ reflection at 21.5° when DR = 48 and 96 (Figure 4), although the spots for $(001)_m$ reflections are still visible in the XRD pattern (Figure 3b). The other monoclinic peaks are too weak to be detected; even the strongest monoclinic peak at 19.5° is only 3% as intense as the orthorhombic $(110)_o$ reflection when DR = 9. However, the presence of $(200)_m$ and $(\bar{2}01)_m$ monoclinic peaks at 23.17 and at 25.11°, respectively, can be inferred from increases in the base width of the orthorhombic peak at 23.95° as DR is increased from 1 to 9 (Figure 4a–c). These results suggest that the orientation (and, perhaps, population) of monoclinic crystals strongly depends on the degree of film extension. The presence of a monoclinic crystal component may also account in part for the lower crystallinities calculated from XRD than from DSC data.

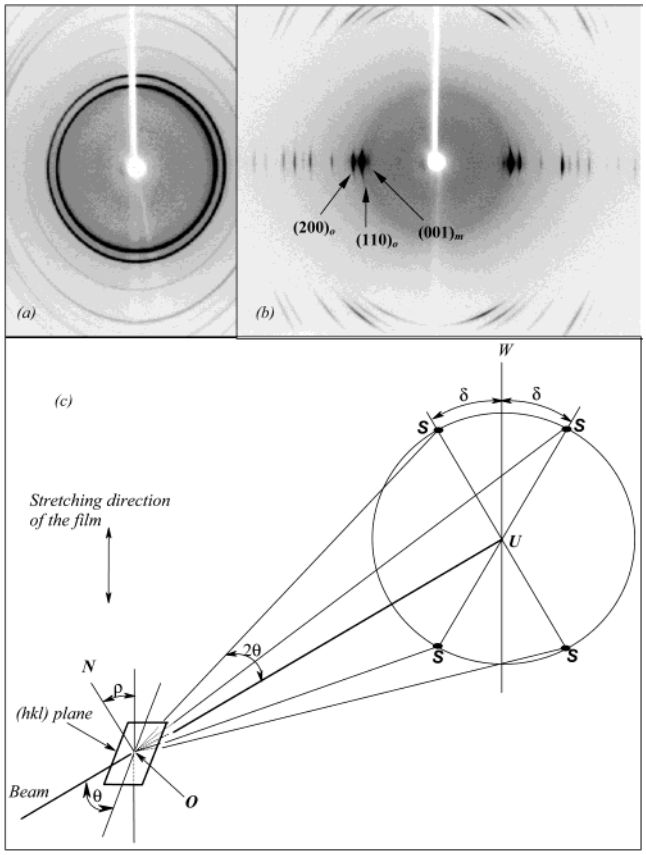

Figure 3. X-ray diffraction patterns of **UHMWPE**: (a) unstretched film and (b) vertically stretched film (DR = 48) as defined in part c, where $(001)_m$ is the reflection from monoclinic planes and $(110)_o$ and $(200)_o$ are reflections from orthorhombic planes; (c) relationship between film geometry (see text) and radial intensity maxima of diffractions. Part c was adapted from ref 29.

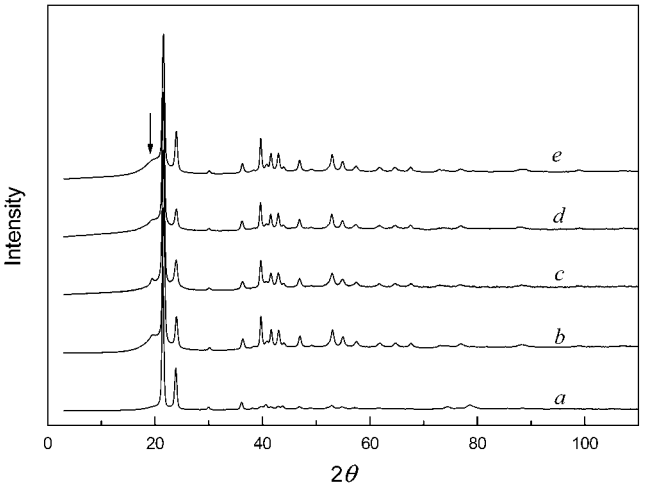

Figure 4. Normalized X-ray diffraction patterns of **UHMWPE**: unstretched film (a) and vertically stretched films (b) DR = 4, (c) DR = 9, (d) DR = 48, and (e) DR = 96. The arrow indicates the position of the monoclinic $(001)_m$ diffraction.

No attempt was made to adjust crystallinities in Table 1 from XRD data to reflect the presence of the monoclinic components.

The angles between orthorhombic planes and the stretching direction can be calculated using the model in Figure 3c in which the X-ray beam is perpendicular to a vertically stretched **UHMWPE** film at ***O*** and diffraction occurs from the (*hkl*) plane to produce four intensity spots on the Debye−Scherrer ring (*S*).[29] *U* is the center of the diffraction rings, *UW* is parallel to the stretching direction of the film, *ON* is the normal to the set of planes with preferred orientation, and ρ is the angle between *ON* and the stretching direction. The relationship between the angles ρ and δ (between *UW* and *US*) is expressed by eq 3. Since $\rho = \delta = 90°$, the planes represented by the equatorial reflections (i.e., $(110)_o$, $(200)_o$, etc.) are parallel to the axis of film stretching. The planes with $l \neq 0$ make angles to the axis of film stretching (Figure 4 of the Supporting Information) that are different from 90°.

$$\cos \rho = \cos \delta \cos \theta \qquad (3)$$

Distribution of Py in UHMWPE films. Partially crystalline polyethylene consists of amorphous parts, the interiors of microcrystals, lateral surfaces of microcrystals, and the near lamellar surfaces of microcrystals (i.e., interfacial regions).[30] The interfacial content usually decreases as the crystallinity increases because microcrystal sizes increase commensurately.[10g] On that basis, the interfacial content of **UHMWPE** must be negligible. Because of the method of preparation of **Py/UHMWPE** films, pyrene molecules are probably distributed between defect sites and the limited amorphous parts, both of which are surrounded by crystalline regions. The shape and size of pyrene molecules make very unlikely their isomorphous incorporation within crystals of **UHMWPE**;[30,31] if they are trapped within a crystalline lattice, they must make their local environment noncrystalline.

Support for this site model is found in the very long periods, more than one month, necessary to remove doped pyrene molecules from unstretched **UHMWPE**, even when films are extracted in hot chloroform, a good swelling solvent for *branched, lower molecular weight* polyethylene.[10c] By contrast, less than 1 week is required to remove all traces of doped pyrene when "normal" polyethylene films are placed in chloroform at room temperature. Thus, the average environments experienced by pyrene molecules (and access to them) in **UHMWPE** and polyethylenes of lower crystallinity and molecular weight must be very different.

Attachment of Pyrene to UHMWPE Chains. Intense UV/vis radiation sources are known to effect attachment of pyrene to alkanes,[31,32] alcohols,[33] and polyethylene chains.[10] At low temperatures, irradiation of **Py** in methane or cyclohexane matrixes at 185 or 248 nm produces as many as four photoproducts, including 1-alkylated pyrenes.[32] When $\lambda > 300$ nm, the efficiency and selectivity of attachment are greater in the solid than in the solution phases of alkanes, and only one photoproduct was detected in the solid phases of *n*-alkanes with ≥21 carbon atoms containing initially [Py] $\lesssim 10^{-5}$ M.[31] At irradiation wavelengths >250 nm, the proposed mechanism of attachment involves sequential absorption of two photons.[10,31,32,33]

The attachment of pyrene to polymers can be achieved also by means of radiolysis involving quanta of fast electrons,[34] γ-rays,[34b,35] or protons[10f] with energies in the MeV range. A fundamental difference between attachments induced by radiolysis and photolysis is the means by which energy enters the systems: photonic mechanisms involve direct excitation of **Py** molecules to electronically excited states; radiolytic methods deposit the vast majority of the energy initially into the solvent matrix, producing initially ions and electrons, as well

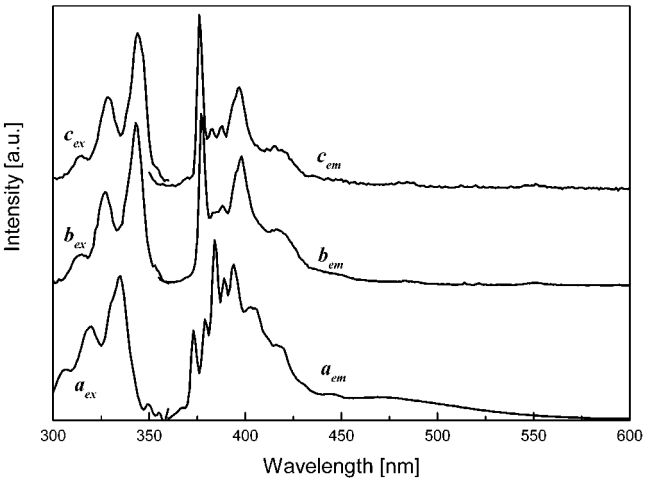

Figure 5. Excitation and emission spectra of unstretched 2.8 $\times$ 10^{-3} mol kg^{-1} **Py/UHMWPE** films before (a_{ex} and a_{em}; λ_{ex} = 336 nm and λ_{em} = 377 nm) and after (b_{ex} and b_{em}; λ_{ex} = 343 nm and λ_{em} = 377 nm) 4.5 MeV proton bombardment and exhaustive extraction with chloroform, and of a **LDPE** film doped with 1.0 $\times$ 10^{-6} mol kg^{-1}1-ethylpyrene (c_{ex} and c_{em}; λ_{ex} = 343 nm and λ_{em} = 377 nm). There is a 1 nm difference between spectra b_{em} and c_{em}.

as electronically excited states of **Py**. Recombination of positive holes with well-trapped electrons can occur subsequently and lead to additional chemical events.[36] The rate of geminate ion-recombination is known to be very dependent on the concentration of pyrene, the viscosity of the medium, and temperature.

(a) 4.5 MeV Proton Bombardment. After bombardment of doped films with 4.5 MeV protons (F = 10^{12} cm^{-2}) and exhaustive extraction with $CHCl_3$ to remove unattached pyrene, no residual pyrene *or* 1-pyrenyl groups were detectable by absorption spectroscopy in the films. However, emission (Figure 5, a_{em}, b_{em}, and c_{em}) and excitation (Figure 5, a_{ex}, b_{ex}, and c_{ex}) spectra demonstrate that some pyrene molecules had been covalently attached at their 1-position to chains of **UHMWPE**: both emission and excitation profiles of the bombarded (and exhaustively extracted) films are different from that of pyrene-doped films, but they are superimposable with that of 1-ethylpyrene in a low-density polyethylene film (**LDPE**);[10b] the emission from the bombarded **Py/UHMWPE** films, **Py-UHMWPE-H**$^+$, is not attenuated upon further extractions with chloroform. Although the emission profiles are invariant when λ_{ex} = 343, 327, and 315 nm, indicating that only chromophore is being excited, a different emission pattern is obtained at λ_{ex} = 352 nm; a small amount of another lumophore besides 1-alkylated pyrene is present.[10b] An upper limit for the concentration of attached 1-pyrenyl groups, 2 $\times$ 10^{-5} mol kg^{-1}, is calculated from absorption spectra assuming a peak at 242 nm with OD > 0.005 could have been detected and a molar extinction at this wavelength equal to that of 1-ethylpyrene in hexane, 79 400 M^{-1} cm^{-1}.[37]

Temporal decays of fluorescence intensity from the **Py-UHMWPE-H**$^+$ film were measured at λ_{em} = 377 and 398 nm and λ_{ex} = 343 nm by the time-correlated single-photon counting (TCSPC) method.[32] The data could be fitted well to equations with three exponential decay constants, discounting a short decay from scatter (Figure 5 of the Supporting Information): at λ_{em} = 377 nm, 180 (89.8%), 40.0 (8.2%), and 3.7 (3.0%) ns; the decay constants are invariant with λ_{em} but the percent of each component varies slightly and the average decay constant, $\langle\tau\rangle$,[38] is 48.5 ns. In low crystallinity polyethylene films, the fluorescence of 1-ethylpyrene, a model for the attached pyrenyl groups, follows a monoexponential decay and $\tau \cong$ 200 ns.[39] TCSPC studies on undoped **UHMWPE** films before bombardment showed a very short-lived scatter peak and an exceedingly weak longer emission that was barely detectable above the noise level. After bombardment of an undoped **UHMWPE** film with the same dose of protons as the **Py/UHMWPE** film, analyses by TCSPC provided two decay constants, 3.5 (87.0%) and 28.8 ns (13.0%) ($\langle\tau\rangle$ = 4.0 ns), as well as a short time decay from scatter. Therefore, the longest decay constant from **Py-UHMWPE-H**$^+$ must be related to interactions between polymer chains and pyrene molecules that lead to covalent attachment; it is attributed to emissions from electronically excited 1-pyrenyl groups that are isolated from other aromatic species.

The other two decays, especially the 3.7 ns component, appear to be due to changes induced in **UHMWPE** by proton bombardment (i.e., chain fragmentation processes that lead subsequently to cross-linking, disproportionation, and creation of unsaturated centers[40]). Minor decay components that are similar in magnitude to the $\sim$ 40 ns decay observed here have been found in films of other polyethylenes to which pyrene was attached,[4b,c] and they have been ascribed tentatively to excimer-like emissions from pairs of neighboring 1-pyrenyl groups.[10a,e,f] To determine whether that is the case here, a proton bombarded **Py-UHMWPE-H**$^+$ film was soaked in xylenes at 110 °C for 4 h, leading to significant swelling and gelation. After the xylenes were removed, TCSPC analyses of the reconstituted film showed the same three component decays as before—183 (87.5%), 42.0 (8.5%), and 4.8 (4.0%) ns; $\langle\tau\rangle$ = 51.9 ns—indicating either that swelling does not increase the mobility of paired pyrenyl groups (due to local cross-links) or that pairs of pyrenyl groups are not present prior to swelling (i.e., the $\sim$40 ns emission is not from an excimeric-like species). The fact that the percentages of each component remain virtually unchanged after swelling is a strong indicator that the $\sim$40 ns emission is not from aggregated 1-pyrenyl groups in this case.

(b) eV Range Photon (>300 nm) Irradiation. As above, no UV/vis absorptions attributable to pyrenyl moieties could be detected from **Py/UHMWPE** films after irradiation with >300 nm photons under vacuum and exhaustive extraction with chloroform, but the corresponding excitation and emission spectra were characteristic of a 1-pyrenyl group. Temporal emission histograms (λ_{ex} = 343 nm; λ_{em} = 377 nm) of the photon-prepared **Py-UHMWPE** film, **Py-UHMWPE-h*ν***, were fitted well to an expression with three exponential decay terms (183 (84.7%), 50.0 (11.4%), and 4.5 (3.9%) ns; $\langle\tau\rangle$ = 52.7 ns) that are similar in magnitude and importance to those from the **Py-UHMWPE-H**$^+$ film.

Irradiations of unstretched **Py/UHMWPE** films were also performed under an N_2 atmosphere to determine whether traces of oxygen affect the attachment processes as they do in other **PE** films.[10i] A **Py/UHMWPE** film was cut into two, and one piece was irradiated under an N_2 atmosphere while the other was irradiated in an identical fashion under vacuum. Surprisingly, no clear differences in the spectral and emission decay properties of the two **Py-UHMWPE-h*ν*** films were discernible; the decay constants (after removal of unattached pyrene) are 187 (77.5%), 46.2 (19.8%) ,and 6.3

Table 2. Linear Dichroic Parameters of Pyrene Molecules in Unstretched and Stretched Polyethylene Films

film	draw ratio	$D_{ld,y}$	$K_{ori,y}$	$D_{ld,z}$	$K_{ori,z}$
UHMWPE	1	0.99 ± 0.05	0.33 ± 0.01	0.96 ± 0.07	0.33 ± 0.01
	9	0.99 ± 0.06	0.33 ± 0.01	1.61 ± 0.10	0.44 ± 0.02
	96	1.02 ± 0.20	0.34 ± 0.04	1.47 ± 0.26	0.42 ± 0.05
LDPE[a]	5		0.32		0.50

[a] Reference 42c.

ns (2.7%) ($\langle\tau\rangle$ = 51.8 ns) from irradiation under N_2 and 193 (84.1%), 36.0 (12.4%), and 3.1 (3.5%) ns ($\langle\tau\rangle$ = 50.5 ns) from irradiation under vacuum.

A highly stretched (DR = 96) **Py/UHMWPE** film was also irradiated at > 300 nm under vacuum. Removal of unattached pyrene molecules from this film was exceedingly difficult. As indicated by the excitation spectra (Figure 6 of the Supporting Information), the excitation spectral bands from primarily attached 1-pyrenyl groups (at 343, 327, and 314 nm) contain vestiges of bands from (unattached) pyrene molecules (at 336, 321, and 308 nm) even after 60 days of extraction! Ultra-stretching **UHMWPE** films orients and extends polyethylene chains while entrapping pyrene molecules in sites surrounded by crystalline domains that are resistant to intrusion by swelling agents.

Linear Dichroism Spectra of Stretched Py/UHMWPE Films. Stretched polyethylene films are commonly used to orient aromatic molecules[41,42] or dichroic dyes.[3g,43] Complete orientational analyses assume that film stretching is uniaxial and require that there be at least some spectral features uniquely polarized along one molecular axis.[42] Linear dichroic studies are limited here to stretched **Py/UHMWPE** films because of the exceedingly low optical densities in the near UV/vis range of **Py-UHMWPE** films even before stretching.

Consistent with the mode of preparation of unstretched **Py/UHMWPE** films, their absorption spectra are indistinguishable in shape and intensity when the direction of linearly polarized light is changed by 90°—pyrene molecules are randomly oriented within the film. The corresponding stretched (DR = 9) film provides $OD_{\parallel}$ and $OD_{\perp}$ spectra (Figure 7 of the Supporting Information) from which the dichroic ratios, D_{ld}, and orientation factors, K_{ori}, (eqs 4 and 5) can be calculated.[44] The indices *i* refer to the long (*z*) and short (*y*) in-plane molecular axes of pyrene. The absorption at 337 nm (*z*-polarized;$^1D_{b1g\rightarrow au}$ transition) provides an excited state with B_{1u} symmetry and that at 274 nm (*y*-polarized; $^1D_{b1g\rightarrow 3u} + {}^1D_{b2g\rightarrow au}$ transitions) with B_{2u} symmetry.[41,42,44]

$$D_{ld,i} = (OD)_{i,\parallel}/(OD)_{i,\perp} \quad (4)$$

$$K_{ori,i} = D_{ld,i}/(D_{ld,i} + 2) \quad (5)$$

$K_{ori,y}$ values of stretched **Py/UHMWPE** films at 9 and 96 draw ratios are near that of the unstretched film. Orientation factors of most (*but not all*) organic molecules can be explained in terms of their shapes.[44,45] The "orientation triangle", in which each orientation distribution is represented by a point with coordinates $K_{ori,z}$, $K_{ori,y}$ (Figure 6),[41,42,44] is a simple method to relate molecular structures and orientations. The vertexes of the "orientation triangle" ($^1/_3$, $^1/_3$) represent a totally random orientation of ball-like molecules, while perfect alignments of the *yz* molecular planes of disklike molecules and the molecular *z*-axis rodlike molecules are found at ($^1/_2$, $^1/_2$) and (0, 1), respectively. Because the aspect ratio of the molecular axes of pyrene is smaller than that of rodlike **1** and larger than that of disklike **3**, $K_{ori,z}$ and $K_{ori,y}$ of pyrene in stretched **LDPE** are intermediate between those of **1** and **3**.[46] $K_{ori,z}$ of pyrene is somewhat *lower* in stretched **UHMWPE** than in stretched **LDPE**. In contrast, a much more elongated molecule has been found to have a dichroic ratio of 30 in highly drawn **UHMWPE**[3g]. We believe that the unexpectedly low value of $K_{ori,z}$ in **UHMWPE** (Figure 6 and Table 2) can be explained by the molecular shape of pyrene and the model suggested above for the sites in which it resides.

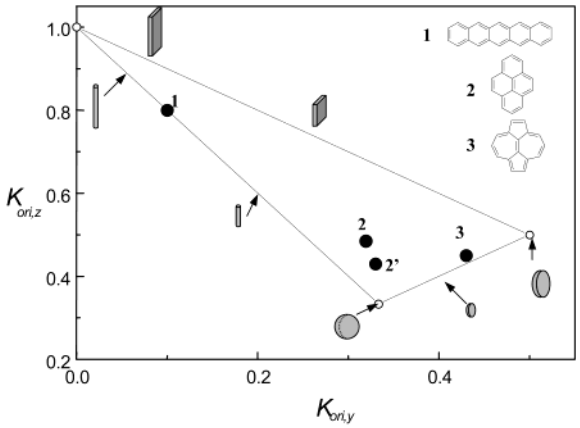

Figure 6. Orientation factors of pyrene in a stretched (DR = 9) **UHMWPE** film (**2′**) and of pyrene (**2**) and other aromatic molecules in stretched **LDPE** films.[42b,c] The figure was adapted from ref 42b.

The spherulitic organization of **LDPE** microcrystals is transformed by film stretching into pieces that are oriented along the extended axis, *but the lamellar organization within the microcrystals is maintained*.[47] Guest molecules like pyrene preferentially occupy interfacial sites (i.e., between the lateral faces of lamellae and amorphous chains) after film stretching;[30,42c,d] pyrene molecules are sandwiched between lamellar folded chains on one face and less well organized amorphous chains on the other. Chains of unstretched **UHMWPE** films (from gel preparations) are packed into lamellae, also. However, the chains unfold when **UHMWPE** films are drawn and become extended along the axis of stretching. As a result, there are few, if any, interfacial sites like those in stretched **LDPE**. The orientation data indicate that pyrene molecules occupy "defect" sites in which their shape distorts the preferred organization of neighboring polyethylene chains even though chains slightly more distant from both faces of pyrene molecules may be fully extended. Such sites may be incapable of orienting pyrene molecules because of their local "amorphous" nature. Thus, the consequences of film stretching differ enormously between the two film types, and the orientation of polyethylene chains in crystalline regions are, on average, either *perpendicular* (stretched **LDPE**)[47] or *parallel* (stretched **UHMWPE**) to the draw direction. $K_{ori,z}$ values of pyrene in **LDPE** films increase from 0.33 (i.e., randomly oriented) at 0% crystallinity to 0.55 at 24% crystallinity, and

Table 3. Partitioning Constants (K_{par}) for DMA (initially 0.95 M in Methanol) in Stretched (DR = 9) and Unstretched Py-UHMWPE-h*ν* Films and in Other Unstretched PE Films at 25 °C[10g]

film type	T (°C)	$K_{par}^{unstretched}$	$K_{par}^{stretched}$
	13.5	0.23 ± 0.03	0.09 ± 0.02
	18.0	0.22 ± 0.03	0.11 ± 0.02
Py-UHMWPE-h*ν*	25.0	0.21 ± 0.03	0.12 ± 0.03
	35.0	0.23 ± 0.02	0.11 ± 0.03
	45.0	0.23 ± 0.02	0.15 ± 0.04
	65.0	0.19 ± 0.03	0.11 ± 0.03
PE22	25	0.29 ± 0.01	
PE35	25	0.20 ± 0.01	
PE38	25	0.26 ± 0.01	
PE42	25	0.27 ± 0.01	
PE73	25	0.21 ± 0.01	

remain near that value as crystallinity is further increased;[48] The lower orientation factor for pyrene in stretched **UHMWPE** films, 0.43, is indicative of the differences between the microstructures of **LDPE** and **UHMWPE**.

DMA Diffusion Studies in Stretched (DR = 9) and Unstretched Py-UHMWPE-h*ν* Films. Partitioning of **DMA** is considered complete when the pyrenyl fluorescence intensity ceases to decrease perceptibly for **Py-UHMWPE** films immersed in **DMA**/methanol solutions.[10a,c,g] Methanol is used here because it solubilizes **DMA** but does not enter **PE** films.[10a−c,h] Although K_{par} of **LDPE** films are known to be temperature dependent,[10c] those for both unstretched and stretched **Py-UHMWPE-h*ν*** films are not within the range investigated (Table 3).[10g] Since K_{par} values for unstretched **Py-UHMWPE-h*ν*** films are about twice as large as the values of the stretched (DR = 9) film, mean free volume per site in the latter film must be smaller than in the unstretched film; from positron annihilation spectroscopy, the mean free volumes are calculated to be 126 Å^3.[49] Somewhat surprisingly, K_{par} for *unstretched* **UHMWPE** and **LDPE** films are comparable at room-temperature despite the mean free volume and site concentration of **UHMWPE** being smaller than those of **LDPE**.[50] However, K_{par} values in unstretched and stretched **LDPE** films are similar.[10c,50] Destruction of lamellae and extension of polyethylene chains upon stretching **UHMWPE** have important influences on the pathways for **DMA** entry. The data suggest that interfaces between lamellae constitute the preferential diffusional pathway for **DMA** molecules in unstretched **UHMWPE**.

After immersion of **Py-UHMWPE-h*ν*** films in N_2-saturated 0.95 M **DMA**/MeOH solutions at constant temperature for long periods (1−2 days), a new, broad emission appears at 400−500 nm (Figure 7a) that is associated with exciplexes between **DMA** and pyrenyl groups; excitation spectra monitored at 450 nm (or 377 nm; not shown) retain the characteristic peaks of 1-pyrenyl groups, but there is some distortion due to the competitive absorption and emission by **DMA** (Figure 7b). The lower *relative* intensity in the 400−500 nm emission region for the stretched (DR = 9) **Py-UHMWPE-h*ν*** film is consistent with the lower **DMA** concentrations noted above.

Decay constants from TCSPC experiments (λ_{ex} 343 nm; λ_{em} 377 nm) for unstretched (181 (57%), 61.1 (23%), and 11.8 ns (20%); $\langle\tau\rangle$ = 41.4 ns) and stretched (DR = 9) (182 (79%), 61.2 (17%), and 7.3 ns (4%); $\langle\tau\rangle$ = 50.4 ns) **DMA**-saturated **Py-UHMWPE-h*ν*** films were very similar to those from **DMA**-free films, but the percentage of each component was different, especially in the case of the unstretched film. Comparison of both the magnitudes and percentages of decay constants from the stretched **Py-UHMWPE-h*ν*** film before (vide ante) and after equilibration with **DMA** demonstrate that a significant portion of the 1-pyrenyl groups is inaccessible to **DMA** despite the fact that the quencher concentration in the film, ca. 0.1 mol kg^{-1}, is sufficient to quench a large fraction of 1-pyrenyl groups attached to other types of **PE** films.[10a−e] In addition, decay constants have been determined in the **DMA**-saturated films when λ_{em} is 450 nm (λ_{ex} 343 nm): 181 (22%), 87.2 (62%), and 12.3 ns (16%) ($\langle\tau\rangle$ = 45.3 ns) when unstretched and 182 (37%), 92.6 (55%), and 8.1 ns (8%) ($\langle\tau\rangle$ = 49.9 ns) when stretched. Consistent with the attribution of this emission primarily to an exciplex, the decay constants of intermediate value are somewhat longer and of much greater importance than when λ_{em} = 377 nm.

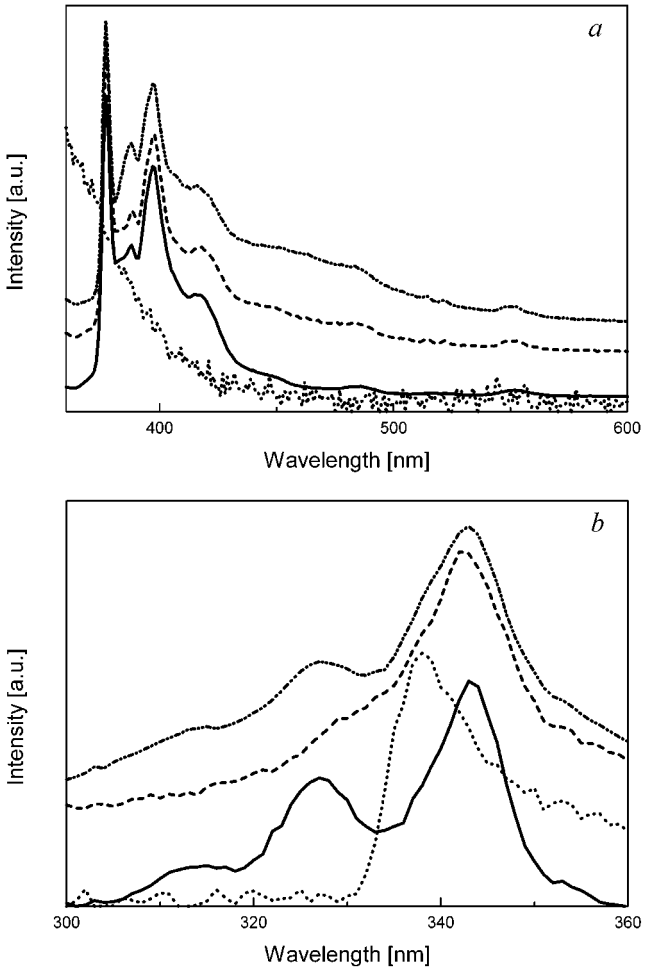

Figure 7. Normalized emission (a, λ_{ex} 343 nm) and excitation (b, λ_{em} 450 nm) spectra of degassed samples: **DMA** (...), unstretched **Py-UHMWPE-h*ν*** in the absence (—) and presence (- - -) of **DMA**, and stretched (DR = 9) **Py-UHMWPE-h*ν*** in the presence of **DMA** (— .. —). In all cases, the **DMA** was 0.95 M in methanol, and films were immersed in the solutions for 2 days at room temperature prior to recording spectra.

Diffusion of small molecules has been employed previously to explore the microstructures of several polymer types,[9a,51] including polyethylenes,[10a−d,52] but not **UHMWPE**. To measure in-diffusion rates and calculate the related diffusion constants (D),[10a−e,g,h] **Py-UHMWPE-h*ν*** films were immobilized and immersed in N_2-saturated 0.95 M **DMA**/MeOH solutions at constant temperature while the *decrease* in the intensity

Table 4. Coefficients (D, cm^2 s^{-1}) and Other Parameters (See Text) for DMA Diffusion (from Methanol) within Unstretched Py-UHMWPE-hν and Other Unstretched PE Films[10g]

			in-diffusion			out-diffusion		
film type	T (°C)	Φ_q (%)[a]	α_{in}	$10^{10}D_{in1}$	$10^{9}D_{in2}$	α_{out}	$10^{10}D_{out1}$	$10^{9}D_{out2}$
Py-UHMWPE-hν	13.5	38	0.37 ± 0.03	0.43 ± 0.10	0.67 ± 0.03	0.55 ± 0.03	0.71 ± 0.15	0.67 ± 0.41
	15.7	39	0.33 ± 0.04	1.05 ± 0.07	0.95 ± 0.11	0.51± 0.04	0.99 ± 0.37	2.01 ± 0.90
	21.6	34	0.25 ± 0.03	4.06 ± 0.42	1.95 ± 0.31	0.53 ± 0.04	3.17 ± 2.10	3.46 ± 1.07
	24.7	37	0.27 ± 0.02	2.86 ± 0.37	2.47 ± 0.15	0.47 ± 0.17	4.23 ± 1.61	4.09 ± 2.53
	30.0	44	0.34 ± 0.19	5.83 ± 4.20	6.39 ± 0.93	0.38 ± 0.05	5.65 ± 2.49	5.62 ± 2.91
	30.2	38	0.31 ± 0.15	12.7 ± 3.2	4.57 ± 0.55	0.34 ± 0.09	7.62 ± 2.01	6.92 ± 2.53
	35.3	40	0.32 ± 0.08	18.0 ± 6.3	8.03 ± 3.20	0.29 ± 0.06	8.75 ± 4.56	7.02 ± 2.50
	37.6	30	0.24 ± 0.26	10.8 ± 6.30	4.94 ± 3.25	0.48 ± 0.14	12.4 ± 3.7	12.0 ± 4.30
	45.0	42	0.20 ± 0.08	27.6 ± 5.2	24.8 ± 5.70	0.45 ± 0.19	36.7 ± 7.3	34.2 ± 9.4
	49.5	36	0.17 ± 0.08	41.6 ± 10.1	46.2 ± 8.1	0.36 ± 0.20	53.0 ± 12.1	51.3 ± 9.0
	59.5	44	0.08 ± 0.11	99.2 ± 15.6	87.3 ± 12.1	0.26 ± 0.13	108.2 ± 15.1	91.4 ± 11.1
PE29	25		*b*		5.51 ± 0.05			6.02 ± 0.09
PE35	25		*b*		8.24 ± 0.02			
PE38	25		*b*		8.68 ± 0.03			9.23 ± 0.02
PE42	25		*b*		7.21 ± 0.02			6.81 ± 0.01
PE73	25		0.19	0.92 ± 0.07	1.68 ± 0.02	0.14	0.83 ± 0.01	1.98 ± 0.03

[a] ±1%. [b] One diffusion coefficient needed for analysis.

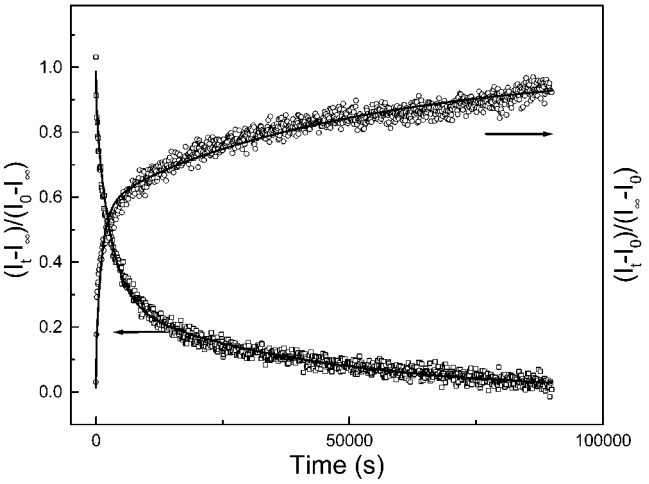

Figure 8. Fluorescence intensity changes during **DMA** diffusion in to and out from an unstretched **Py-UHMWPE-hν** film at 13.5 °C: (□) in-diffusion, film immersed in 0.95 M **DMA** in methanol solution; (○) out-diffusion, film immersed in neat methanol.

of their pyrenyl fluorescence was monitored as a function of time (Table 4 and Figure 8). The period required to reach maximum pyrenyl fluorescence quenching (i.e., equilibrium **DMA** concentrations) decreases as temperature is increased. For instance, only 60 min are required at 45.0 °C but 23 h are needed at 15.7 °C using unstretched **Py-UHMWPE-hν**. The apparent lack of temperature dependence on the amount of pyrenyl fluorescence quenched by **DMA** at equilibrium, Φ_q (=100[1 − I_∞/I_0], where I_0 and I_∞ are the fluorescence intensities at time = 0 and at equilibrium, respectively), suggests that some pyrenyl groups are located in crystalline sites not accessible to **DMA**; there is no "amorphous path" to them. Out-diffusion rates were obtained by placing the **DMA**-saturated film into neat methanol and measuring the *increase* in fluorescence intensity of the pyrenyl emission as a function of time (Table 5).

At any time t, C_t/C_0, the fraction of pyrenyl groups with at least one **DMA** molecule as a neighbor within a film, should be equal to the fraction of pyrenyl excited singlet states that are quenched by **DMA**. In terms of fluorescence intensities, the latter fraction is equal to $(I_t - I_\infty)/(I_0 - I_\infty)$,[13] where I_t is the fluorescence intensity at time = t and I_0 is obtained from the intercept of the slope of the linear region of a plot of fluorescence intensity vs $t^{1/2}$.[10b,g] In this way, the fluorescence data for in-diffusion and out-diffusion of **DMA** can be treated according to integrated forms of Fick's second law, eqs 6 and 7,[10g,13,53] respectively, in which l is the film thickness (cm) and D has units of cm^2 s^{-1}.

Unlike the case in unstretched **LDPE** films (N. B., **PE** with less than 50% crystallinity; see Table 4),[10b,h] two diffusion coefficients, D_1 and D_2, are required to fit well the **DMA** diffusion data in unstretched **Py-UHMWPE-hν** films. The term α is the fraction of diffusion occurring via the D_1 process. The best fit was achieved by adjusting the value of α empirically so that the difference, $\sum|I_t - I_t^{fit}|^2$, was minimized.

$$\frac{I_t - I_\infty}{I_0 - I_\infty} = \alpha\frac{8}{\pi^2}\sum_{n=0}^{15}\frac{1}{(2n+1)^2}e^{(-D_1(2n+1)^2\pi^2 t/l^2)} + (1-\alpha)\frac{8}{\pi^2}\sum_{n=0}^{15}\frac{1}{(2n+1)^2}e^{(-D_2(2n+1)^2\pi^2 t/l^2)} \quad (6)$$

$$\frac{I_t - I_\infty}{I_0 - I_\infty} = 1 - \alpha\frac{8}{\pi^2}\sum_{n=0}^{15}\frac{1}{(2n+1)^2}e^{(-D_1(2n+1)^2\pi^2 t/l^2)} - (1-\alpha)\frac{8}{\pi^2}\sum_{n=0}^{15}\frac{1}{(2n+1)^2}e^{(-D_2(2n+1)^2\pi^2 t/l^2)} \quad (7)$$

The diffusion coefficients, $(D_{in})_i$ and $(D_{out})_i$, for in- and out-diffusion of **DMA** in unstretched films tend to increase with temperature, as expected, but the values change somewhat erratically. We suspect that variations in the thickness along the surface of one film are responsible in large part for the inconsistencies. At ca. 25 °C, the diffusion constants of **DMA** in unstretched **Py- UHMWPE-hν** are less than half the values in unstretched **LDPE** films but are near those in a high-density film, **PE73** (Table 4). Since two D values are also necessary to fit the diffusion data for **DMA** in unstretched **PE73**, a "normal" **PE** of high crystallinity, the complex diffusional behavior may be related to the high degree of crystallinity.

Activation energies for **DMA** diffusion in the unstretched **Py-UHMWPE-hν** films have been calculated from Arrhenius-like plots of the D values (Figure 9). The

Table 5. Diffusion Coefficients ($cm^2\ s^{-1}$) of DMA (from Methanol) within Stretched (DR = 9) Py-UHMWPE-h*ν*

		in-diffusion			out-diffusion		
T (°C)	Φ_q (%)[a]	α_{in}	$10^{10}D_{in1}$	$10^{9}D_{in2}$	α_{out}	$10^{10}D_{out1}$	$10^{9}D_{out2}$
17.4	20	0.53 ± 0.15	1.01 ± 0.44	1.56 ± 0.41	0.49 ± 0.17	1.73 ± 0.15	2.38 ± 0.37
21.5	22	0.43 ± 0.09	2.31 ± 0.06	2.56 ± 0.12	0.54 ± 0.17	3.51 ± 0.03	5.19 ± 0.19
24.0	19	0.39 ± 0.09	2.23 ± 0.98	3.47 ± 0.92	0.46 ± 0.15	3.51 ± 0.57	4.55 ± 0.95
29.6	24	0.41 ± 0.05	4.32 ± 1.70	6.02 ± 0.56	0.34 ± 0.06	5.40 ± 1.11	7.49 ± 1.77
32.1	23	0.33 ± 0.02	5.48 ± 1.44	5.24 ± 0.82	0.53 ± 0.09	7.55 ± 2.25	8.90 ± 2.44
34.9	25	0.31 ± 0.08	8.02 ± 3.02	6.56 ± 2.38	0.46 ± 0.11	10.5 ± 2.89	9.23 ± 2.21
39.5	27	0.25 ± 0.06	11.1 ± 2.3	8.78 ± 1.33	0.34 ± 0.08	10.7 ± 2.8	16.2 ± 3.4
40.6	25	0.26 ± 0.07	10.4 ± 6.4	9.75 ± 0.99	0.32 ± 0.07	11.9 ± 5.4	14.2 ± 2.2
51.7	30	0.23 ± 0.04	20.1 ± 5.4	31.6 ± 5.9	0.30 ± 0.09	26.7 ± 6.2	38.4 ± 7.2
62.1	29	0.16 ± 0.08	52.4 ± 8.8	66.9 ± 11.2	0.22 ± 0.21	62.7 ± 9.6	54.0 ± 12.1

[a] ±1%.

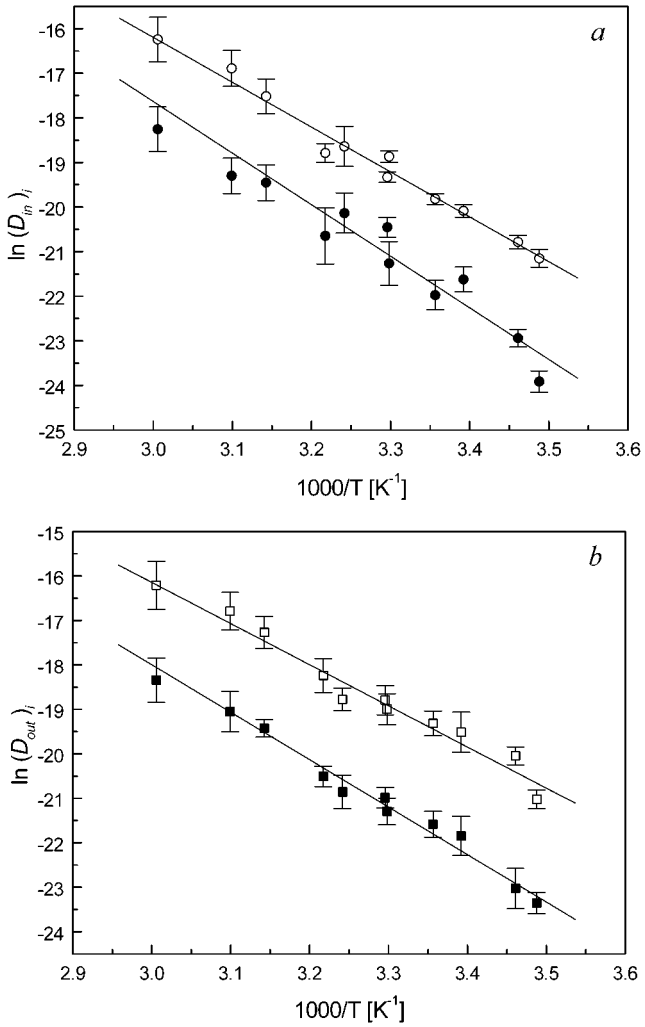

Figure 9. $\ln(D_{in})_i$ (a: $i = 1$ (●); $i = 2$ (○)) and $\ln(D_{out})_i$ (b: $i = 1$ (■); $i = 2$ (□)) vs $1/T$ plots for **DMA** diffusion in an unstretched **Py-UHMWPE-h*ν*** film.

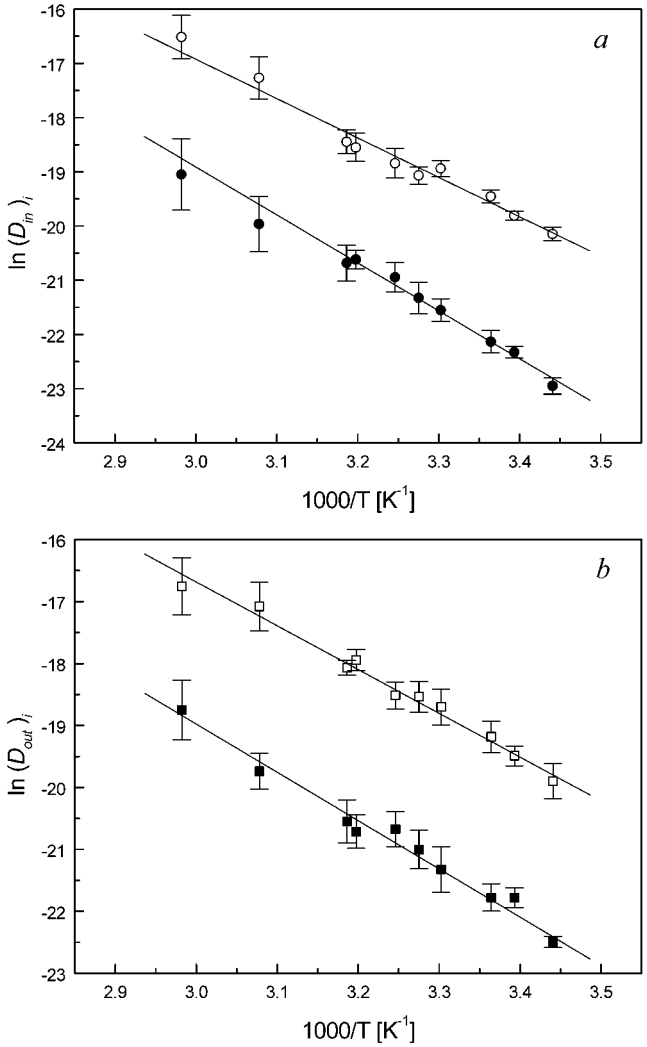

Figure 10. $\ln(D_{in})_i$ (a: $i = 1$ (●); $i = 2$ (○)) and $\ln(D_{out})_i$ (b: $i = 1$ (■); $i = 2$ (□)) vs $1/T$ plots for **DMA** diffusion in a stretched (DR = 9) **Py-UHMWPE-h*ν*** film.

processes with smaller diffusion coefficients have higher activation energies, 96.8 ± 13.2 (in) and 89.0 ± 7.7 kJ mol^{-1} (out), than those of the larger diffusion coefficients, 84.0 ± 7.9 (in) and 76.5 ± 6.8 kJ mol^{-1} (out). However, each of the activation energies in **UHMWPE** is higher than in **LDPE**.[10c,h]

Two diffusion coefficients are also necessary to fit the diffusion data from stretched (DR = 9) **Py-UHMWPE-h*ν*** films (Table 5). The fact that Φ_q of stretched (DR = 9) **Py-UHMWPE-h*ν*** is only half as large as in the unstretched film may be related to the lower D values calculated for the stretched film. The proposed explanations for these phenomena, loss of lamellar−lamellar interfaces and trapping of pyrenyl groups in sites that are virtually inaccessible to a small, diffusing molecule like **DMA**, have been discussed above.

Activation energies for the diffusion processes of **DMA** in the stretched film, 73.5 ± 8.2 and 60.1 ± 5.1 kJ mol^{-1} (in) and 64.8 ± 5.6 and 59.0 ± 3.7 kJ mol^{-1} (out) have been calculated also from Arrhenius-type plots of the diffusion coefficients (Figure 10). Surprisingly, the stretched values are somewhat lower than the unstretched ones and approach the values reported in **LDPE** films.[10a−d] These data should be interpreted not only in terms of the allowed motions of **DMA** molecules

in stretched and unstretched **UHMWPE**, but also remembering that the Φ_q values of the stretched **UHMWPE** film are only about half those of the unstretched film—the diffusion coefficients and activation energies in the stretched films are based on events occurring in a much smaller fraction of the total film volume than in the unstretched film. Apparently, stretching makes some of the previously accessible sites inaccessible to **DMA**. Although the activation energies in the unstretched and stretched films are difficult to compare directly, it appears that the pyrenyl-occupied sites that remain accessible are linked to the film surfaces either by a shorter distance or by more disturbed polymer chains, on average, than accessible sites in the unstretched film.

Conclusions

The packing of chains in unstretched and stretched **UHMWPE** films has been examined in great detail by X-ray diffraction and the results have been correlated with measurements by differential scanning calorimetry. Stretching films of **UHMWPE** has a marked effect on their degree of crystallinity, the orientation and packing of their polymer chains, and the diffusional characteristics of a small molecule, *N*,*N*-dimethylaniline, within a film, but it does not lead to enhanced orientation of another guest molecule, pyrene. Due in part to the gel technique used to prepare the doped films and, perhaps, in part to the intrinsic nature of **UHMWPE**, the pyrene molecules are sequestered tightly in sites that discourage escape or entry by other species. Using the fluorescent properties of attached pyrenyl groups as a diagnostic and marker, it has been possible to demonstrate that the in- and out-diffusion of *N*,*N*-dimethylaniline in **UHMWPE** is less facile and more complicated than in polyethylenes of lower crystallinity. As with other types of polyethylene films of lower crystallinity, pyrene can be attached covalently to **UHMWPE** films upon irradiation with UV/vis (eV range) photons or by bombardment with MeV range protons. However, the mode of preparation of our pyrene-doped **UHMWPE** films, in combination with their intrinsic properties, allows the photoattachment processes to proceed under nitrogen atmospheres with greater selectivity than when other forms of polyethylene are employed. Bombardment of **UHMWPE** films with 4.5 MeV protons also results in cross-linking of chains, as evidenced by differential scanning calorimetry measurements.

Fluorescence from attached pyrenyl groups provides a convenient molecular probe of *local* static (structural) and dynamic (diffusional) changes that occur within **UHMWPE** and should facilitate studies of its wear and durability that have been difficult heretofore.[3b−f,54] For instance, the surprising lack of exceptional orientation of pyrene molecules within the matrices of **UHMWPE** films demonstrates that the microcavities where such guest molecules reside are far different from the bulk structure and that chains in the vicinity of guest molecules are very sensitive to their steric influences.

Acknowledgment. R.G.W. is grateful to the National Science Foundation for financial support. Mr. Gerald O. Brown and Mr. Oliver Schurr are thanked for their assistance with aspects of this work. Dr. Eric B. Sirota is thanked for his advice concerning the XRD data.

Supporting Information Available: Figures showing UV−vis spectra of **Py/UHMWPE** films, DSC thermograms of stretched and unstretched, native, and proton-bombarded **UHMWPE**, the X-ray diffractogram of stretched (DR = 4, 9, 96), unbombarded **UHMWPE** films, the TCSPC histogram of a **Py-UHMWPE-H**$^+$ film, the excitation spectra of a stretched (DR = 96) **Py-UHMWPE-h*ν*** film after extraction in refluxing chloroform for different periods, and linear polarization spectra of a **Py/UHMWPE** film with DR = 9 and a table of X-ray diffraction peaks from a stretched (DR = 48) **UHMWPE** film and their assignments. This material is available free of charge via the Internet at http://pubs.acs.org.

References and Notes

(1) (a) Zwijnenburg, A.; Pennings, A. J. *Colloid Polym. Sci.* **1976**, *254*, 868. (b) Ward, I. M. *Macromol. Symp.* **1995**, *100*, 1. (c) Fan, Z. Y.; Lan, Q.; Bu, H. S.; Wu, L. H.; Sun, L.; Qian, R. Y.; Chen, S. X.; Men, Y. F.; Jiang, B. Z. *Chin. J. Polym. Sci.* **2001**, *19*, 25.

(2) (a) Schellekns, R.; Bastiaansen, C. *J. Appl. Polym. Sci.* **1991**, *43*, 2311. (b) Lemstra, P. J.; Smith, P. *J. Mater. Sci.* **1980**, *15*, 505. (c) Penning, J. P.; Devries, A. A.; Pennings, A. J. *Polym. Bull. (Berlin)* **1993**, *31*, 243. (d) Al-Hussein, M.; Davies, G. R.; Ward, I. M. *Polymer* **2001**, *42*, 3679.

(3) (a) Rahel', J.; Cernak, M.; Hudec, I.; Brablec, A.; Trunec, D.; Chodak, I. *Czech. J. Phys.* **2000**, *50*, 445. (b) Chodak, I. *Prog. Polym. Sci.* **1998**, *23*, 1409. (c) Barham, P. J.; Keller, A. *J. Mater. Sci.* **1985**, *20*, 2281. (d) Hofste, J. M.; Smit, H. H. G.; Pennings, A. J. *Polym. Bull. (Berlin)* **1996**, *37*, 385. (e) Ananthanarayan, V. T.; Shutov, F. *J. Biomater. Appl.* **2001**, *16*, 139. (f) Kurtz, S. M.; Muratoglu, O. K.; Evans, M.; Edidin, A. A. *Biomaterials* **1999**, *20*, 1659. (g) Bastiaansen, C.; Schmidt, H. W.; Nishino, T.; Smith, P. *Polymer* **1993**, *34*, 3951.

(4) (a) Alderson, K. L.; Evans, K. E. *Polymer* **1992**, *33*, 4435. (b) Kunz, M.; Drechsler, M.; Moller, M. *Polymer* **1995**, *36*, 1331. (c) Hofste, J. M.; vanVoorn, B.; Pennings, A. J. *Polym. Bull. (Berlin)* **1997**, *38*, 485. (d) Ivan'kova, E. M.; Myasnikova, L. P.; Marikhin, V. A.; Baulin, A. A.; Volchek, B. Z. *J. Macromol. Sci. Phys.* **2001**, *B40*, 813. (e) Gerrits, N. S. J. A.; Lemstra, P. J. *Polymer* **1991**, *32*, 1770.

(5) (a) Albert, C. F.; Busfield, W. K.; Pomery, P. J. *Polym. Int.* **1992**, *27*, 285. (b) Tino, J.; Klimova, M.; Chodak, I.; Jacobs, M. *Polym. Int.* **1996**, *39*, 231. (c) Jahan, M. S.; King, M. C.; Haggard, W. O.; Sevo, K. L.; Parr, J. E. *Radiat. Phys. Chm.* **2001**, *62*, 141.

(6) (a) VanderHart, D. L.; Khoury, F. *Polymer* **1984**, *25*, 1589. (b) Hu, W. G.; Boeffel, C.; Schmidt-Rohr, K. *Macromolecules* **1999**, *32*, 1611. (c) Uehara, H.; Matsuda, H.; Aoike, T.; Yamanobe, T.; Komoto, T. *Polymer* **2001**, *42*, 5893.

(7) (a) Wong, W. F.; Young, R. J. *J. Mater. Sci.* **1994**, *29*, 520. (b) Bentley, P. A.; Hendra, P. J. *Spectrochim. Acta A* **1995**, *51*, 2125. (c) Bertoluzza, A.; Fagnano, C.; Rossi, M.; Tinti, A.; Cacciari, G. L. *J. Mol. Struct.* **2000**, *521*, 89.

(8) (a) Hermans, P. H.; Weidinger, A. *J. Polym. Sci.* **1949**, *4*, 709. (b) Challa, G.; Hermans, P. H.; Weidinger, A. *Makromol. Chem.* **1962**, *56*, 169. and references therein. (c) Wasiak, A.; Sajkiwicz, P. *J. Mater. Sci.* **1993**, *28*, 6409. (d) Hsieh, Y. L.; Hu, X. P. *J. Polym. Sci. Pol. Phys.* **1997**, *35*, 623. (e) Hu, X. P.; Hsieh, Y. L. *Polym. J.* **1998**, *30*, 771. (f) Bin, Y. Z.; Ma, L.; Adachi, R.; Kurosu, H.; Matsuo, M. *Polymer* **2001**, *42*, 8125. (g) Seto, T.; Hara, T.; Tanaka, K. *Jpn. J. Appl. Phys.* **1968**, *7*, 31. (h) Bunn, C. W. *Trans. Faraday Soc.* **1939**, *35*, 482.

(9) (a) Winnik, F. M. *Chem. Rev.* **1993**, *93*, 587. (b) Soutar, I.; Swanson, L.; Guillet, J. E.; Takahashi, Y. *Macromolecules* **1991**, *24*, 2815. (c) Tang, B. Z.; Holdcroft, S.; Guillet, J. E. *Macromolecules* **1994**, *27*, 5487. (d) Victor, J. G.; Torkelson, J. M. *Macromolecules* **1988**, *21*, 3490. (e) Gangopadhyay, S.; Pleil, M. W.; Borst, W. L. *J. Lumin.* **1990**, *46*, 359. (f) Johnson, B. S.; Ediger, M. D.; Kitano, T.; Ito, K. *Macromolecules* **1992**, *25*, 873. (g) Riley, J. M.; Alkan, S.; Chen, A. D.; Shapiro, M.; Khan, W. A.; Murphy, W. R.; Hanson, J. E. *Macromolecules* **2001**, *34*, 1797. (h) Biscoglio, M.; Thomas, J. K. *J. Phys. Chem. B.* **2000**, *104*, 475.

(10) (a) Naciri, J.; Weiss, R. G. *Macromolecules* **1989**, *22*, 3928. (b) He, Z. Q.; Hammond, G. S.; Weiss, R. G. *Macromolecules* **1992**, *25*, 1568. (c) Jenkins, R. M.; Hammond, G. S.; Weiss, R. G. *J. Phys. Chem.* **1992**, *96*, 496. (d) Lu, L.; Weiss, R. G. *Macromolecules* **1994**, *27*, 219. (e) Kosa, C.; Danko, M.; Fiedlerova, A.; Hrdlovic, P.; Borsig, E.; Weiss, R. G. *Macro-*

molecules **2001**, *34*, 2673. (f) Brown, G. O.; Guardala, N. A.; Price, J. L.; Weiss, R. G. *J. Phys. Chem. B* **2002**, *106*, 3375. (g) Zimerman, O. E.; Cui, C.; Wang, X.; Atvars, T.; Weiss, R. G. *Polymer* **1998**, *39*, 1177. (h) Taraszka, J. A.; Weiss, R. G. *Macromolecules* **1997**, *30*, 2467. (i) Brown, G. O.; Zimerman, O. E.; Weiss, R. G. To be published.

(11) Karpovich, D. S.; Blanchard, G. *J. Phys. Chem.* **1995**, *99*, 3951.

(12) (a) Birks, J. B. *Photophysics of Aromatic Molecules*; Wiley: New York, 1971. (b) Ugur, S.; Pekcan, O. *Polymer* **2000**, *41*, 1571. (c) Yamazaki, I.; Winnik, F. M.; Winnik, M. A.; Tazuke, S. *J. Phys. Chem.* **1987**, *91*, 4213. (d) Dorrance, R. C.; Hunda, T. F. *J. Chem. Soc., Faraday Tans.* **1972**, *68*, 1312. (e) Kalyanasundaram, K.; Thomas, J. K. *Radiat. Res.* **1974**, *60*, 268. (f) Behera, G. B.; Mishra, B. K.; Behera, P. K.; Panda, M. *Adv. Colloid Interface* **1999**, *82*, 1. (g) Tedeschi, C.; Mohwald, H.; Kirstein, S. *J. Am. Chem. Soc.* **2001**, *123*, 954.

(13) Crank, J. *The Mathematics of Diffusion*, Oxford: London, 1956; p 45.

(14) Perrin, D. D.; Amarego, W. L. F. *Purification of Laboratory Chemicals*, 3rd ed; Pergamon Press: New York, 1988; p 267.

(15) MDI Jade 5 software for X-ray diffraction pattern processing. Materials Data, Inc., Livermore, CA.

(16) van Aerle, N. A. J. M. Doctoral Dissertation, Technical University of Eindhoven, The Netherlands, 1989; p 11.

(17) Perkampus, H.-H. in *UV−Vis Atlas of Organic Compounds*, 2nd ed. (part 2); VCH: New York, 1992.

(18) Stout, G. H.; Jensen, L. H. *Structure Determination*; Macmillan: New York, 1968; p 12.

(19) Price, J. L.; Land, D. J.; Stern, S. H.; Guardala, N. A.; Cady, P. K.; Simons, D. G.; Brown, M. D.; Brennan, J. G.; Stumborg, M. F. *Nucl. Instrum. Methods Phys. Res.* **1991**, *B56−57*, 1014.

(20) Attix, F. H. in *Introduction to Radiological Physics and Radiation Dosimetry*; Wiley: New York, 1986; p 191.

(21) Ziegler, J. F.; Manoyan, J. M. *Nucl. Instrum. Methods B* **1988**, *35*, 215.

(22) Russell, K. E.; Hunter, B. K.; Heyding, R. D. *Polymer* **1997**, *38*, 1409.

(23) Gray, A. P. *Thermochim. Acta* **1970**, *1*, 563.

(24) Penning, J. P.; Pras, H. E.; Pennings, A. J. *Colloid Polym. Sci.* **1994**, *272*, 664.

(25) Hermans, P. H.; Weidinger, A. *Makromol. Chem.* **1961**, *44−46*, 24.

(26) Joo, Y. L.; Han, O. H.; Lee, H.-K.; Song, J. K. *Polymer*, **2000**, *41*, 1355.

(27) Pennings, A. J.; Zwijnenburg, A. *J. Polym. Sci., Polym. Phys. Ed.* **1979**, *17*, 1011.

(28) (a) Dorset, D. L. *Acta Crystallogr.* **1995**, *B51*, 1021. (b) Dorset, D. L. *J. Phys. Chem. B* **2000**, *104*, 10543.

(29) Klug, H. P.; Alexander, L. E. *X-ray Diffraction Procedures for Polycrystalline and Amorphous Materials*, Wiley: New York, 1974**,** Chapter 10.

(30) Phillips, P. J. *Chem. Rev.* **1990**, *90*, 425.

(31) Zimerman, O.; Weiss, R. *J. Phys. Chem. A.* **1999**, *103*, 9794.

(32) (a) Lamotte, M.; Joussot-Dubien, J.; Lapouyade, R.; Pereyre, J. In *Photophysics and Photochemistry above 6 eV*; Lahmani, F., Ed.; Elsevier: Amsterdam, 1985; p 577. (b) Lamotte, M.; Pereyre, J.; Lapouyade, R.; Joussot-Dubien, J. *J. Photochem. Photobiol. A* **1991**, *58*, 225.

(33) (a) Sun, Y. P.; Ma, B.; Lawson, G. E.; Bunker, C. E.; Rollins, H. W. *Anal. Chim. Acta* **1996**, *319*, 379. (b) Pandey, S.; Acree, W. E. *Anal. Chem. Acta* **1997**, *343*, 155. (c) Sun, Y. P.; Ma, B.; Lawson, G. E.; Bunker, C. E.; Rollins, H. W. *Anal. Chim. Acta* **1997**, *343*, 159.

(34) (a) Zhang, G. H.; Thomas, J. K. *J. Phys. Chem.* **1996**, *100*, 11438. (b) Milosavljevic, B. H.; Thomas, J. K. *Radiat. Phys. Chem.* **2001**, *62*, 3. (c) Szadkowskanicze, M.; Mayer, J.; Kroh, J. *Radiat. Phys. Chem.* **1992**, *39*, 23.

(35) Tanaka, M.; Yoshida, H.; Ogasawara, M. *J. Phys. Chem.* **1991**, *95*, 955.

(36) Thomas, J. K. *Chem. Rev.* **1993**, *93*, 301 and references therein.

(37) The value of molar extinction coefficient at 242 nm was determined as (1) measuring the absorbance at 242 nm of DMA/hexanes solutions (4.45×10^{-5}, 8.90×10^{-5}, 1.34×10^{-4}, and 1.78×10^{-4} M) and (2) plotting absorbance via concentration. The slope is the molar extinction coefficient at 242 nm, 79 400 $\pm$ 300 M^{-1} $cm^{-1.}$

(38) Lakowicz, J. R. *Principles of Fluorescence Spectroscopy*, 2nd ed.; Kluwer Academic/Plenum: New York, 1999; p 130.

(39) Zimerman, O. E.; Weiss, R. G. *J. Phys. Chem. A* **1998**, *102*, 5364.

(40) Chapiro, A. *Radiation Chemistry of Polymeric Systems*; Wiley: New York, 1962; Chapter 9.

(41) Thulstrup, E. W.; Michl, J. *J. Phys. Chem.* **1980**, *84*, 82.

(42) (a) Thulstrup, E. W.; Eggers, J. H. *Chem. Phys. Lett.* **1968**, *1*, 690. (b) Thulstrup, E. W.; Michl, J.; Eggers, J. H. *J. Phys. Chem.* **1970**, *74*, 3868. (c) Michl, J.; Thulstrup, E. W.; Eggers, J. H. *J. Phys. Chem.* **1970**, *74*, 3878. (d) Konwerska-Hrabowska, J. *Appl. Spectrosc.* **1985**, *39*, 976.

(43) Tirelli, N.; Amabile, S.; Cellai, C.; Pucci, A.; Regoli, L.; Ruggeri, G.; Ciardelli, F. *Macromolecules* **2001**, *34*, 2129.

(44) Michl, J.; Thuistrup, E. W. *Spectroscopy with Polarized Light*, VCH: New York, 1986.

(45) Bott, C. C.; Kurucsev, T. *J. Chem. Soc., Faraday Trans. 2* **1975**, *71*, 749.

(46) (a) Thulstrup, E. W.; Michl, J. *J. Am. Chem. Soc.* **1982**, *104*, 5594. (b) Michl, J.; Thulstrup, E. W. *Acc. Chem. Res.* **1987**, *20*, 192.

(47) (a) Peterlin, A. *Macromolecules* **1980**, *13*, 777. (b) Aggarwal, S. L.; Tilley, G. P.; Sweeting, O. J. *J. Polym. Sci.* **1961**, *51*, 551.

(48) Wang, C.; Xu, J.; Weiss, R. G. To be published.

(49) Hill, A. J.; Meakin, P.; Luo, C.; Weiss, R. G. To be published.

(50) Gu, W. Q.; Hill, A. J.; Wang, X. C.; Cui, C. X.; Weiss, R. G. *Macromolecules* **2000**, *33*, 7801.

(51) (a) Schlotter, N. E.; Furlan, P. Y. *Polymer* **1992**, *33*, 3323. (b) Regev, O.; Zana, R. *J. Colloid. Interface Sci.* **1999**, *210*, 8. (c) Kook, S. K.; Kopelman, R. *J. Phys. Chem.* **1992**, *96*, 10672. (d) Cicerone, M. T.; Blackburn, F. R.; Ediger, M. D. *Macromolecules* **1995**, *28*, 8224. (e) Kneas, K. A.; Xu, W. Y.; Demas, J. N.; DeGraff, B. A. *Appl. Spectrosc.* **1997**, *51*, 1346. (f) Bjorklund, T. G.; Lim, S. H.; Bardeen, C. J. *J. Phys. Chem. B* **2001**, *105*, 11970. (g) Jeon, S.; Bae, S. C.; Granick, S. *Macromolecules* **2001**, *34*, 8401. (h) Beckman, I. N. *Thermochim. Acta* **1991**, *190*, 1. (i) Miguel, M. D. *Adv. Colloid Interface* **2001**, *89*, 1.

(52) Talhavini, M.; Atvars, T. D. Z.; Schurr, O.; Weiss, R. G. *Polymer* **1998**, *39*, 3221.

(53) Comyn, J. *Polymer Permeability*; Elsevier: London, 1985; Chapter 1.

(54) (a) Boontongkong, Y.; Cohen, R. E.; Spector, M.; Bellare, A. *Polymer* **1998**, *39*, 6391. (b) Yim, C. I.; Lee, K. J.; Jho, J. Y.; Choi, K. W. *Polym. Bull. (Berlin)* **1999**, *42*, 433.

MA020235Q